Particle Swarm Optimization for Advanced Tolerance Control in Freeform Geometries: Case Study on Aeronautical Turbine Blades

[1] Oubrek Mohamed [1], *Bellat* Abdelouahad [1,*] , *Salih* Abdelouahab[1] and *Jalid* abdelilah
[1]Mohammed V University in Rabat ENSAM Rabat, PCMT Laboratory Royal Army Avenue, 10100 Rabat, Morocco

Abstract. This research presents an innovative methodology for optimizing geometric tolerances on freeform surfaces, with a particular focus on turbine blades, through the adoption of a global tolerance framework. In contrast to conventional approaches that rely on multiple localized tolerances, the proposed method introduces a unified model aimed at reducing design complexity while ensuring both functional reliability and cost-effectiveness. The case study is based on a turbine blade reconstructed from 3D-scanned point cloud data. The reconstructed geometry was evaluated to characterize deviation distributions, which were then incorporated into a global tolerance model. Genetic algorithms were employed to optimize tolerances, striking a balance between manufacturing costs and performance requirements. The findings reveal significant improvements in quality control efficiency, achieving up to a 20% reduction in manufacturing costs while maintaining aerodynamic and structural integrity. This study underscores the potential of global tolerance strategies to revolutionize tolerance allocation in sectors such as aerospace and energy, where freeform geometries are widely used. By integrating optimization techniques with advanced surface analysis, the approach provides a forward-looking pathway toward greater manufacturing precision and efficiency.

Keywords: Global Tolerance, Turbine Blades, Optimization, Genetic Algorithm, Freeform Surface Analysis, Manufacturing Efficiency.

1 Introduction

In contemporary manufacturing environments—particularly within automotive and aeronautical industries—the conception and validation of freeform geometries remain among the most complex engineering challenges. These surfaces demand precise dimensional definitions to ensure functionality, reliability, and seamless assembly. Conventional design methods typically involve assigning numerous local tolerances to individual features, which often multiplies complexity and increases costs throughout the design, production, and inspection stages [1-2].

To overcome these limitations, researchers and engineers have explored the transition from multiple discrete tolerances to a single, holistic shape tolerance. This global approach provides a unified framework that encapsulates the overall geometric deviations of a component's surface. By optimizing tolerances in this way, manufacturers gain improved control over both critical and secondary areas, achieving higher precision and reducing variability without unnecessary design overhead [3-4].

In the automotive domain, parts such as exterior panels, bumpers, and aerodynamic attachments typically exhibit freeform surfaces. Their dimensional integrity directly affects both aesthetics and performance, influencing parameters such as drag reduction and structural

alignment [5]. Traditional tolerance definitions for these parts can involve dozens of local constraints and checkpoints. The adoption of a global shape tolerance simplifies this process: fewer measurements are required to assess conformity, and tolerance distributions can be tailored—tightened for key functional zones such as mounting interfaces and relaxed for less critical aesthetic surfaces [6-7].

Similarly, in aeronautical applications, freeform geometries are central to turbine blades, wing sections, and fuselage panels. The aerodynamic efficiency of these components relies on maintaining specific geometric contours [8]. In turbine blades, for example, the leading and trailing edges represent high-priority regions, as even minor deviations can affect airflow, efficiency, and safety. Conversely, the mid-sections of the blades can tolerate limited variation without degrading performance. The implementation of optimized shape tolerances allows for resource allocation where precision is essential, reducing inspection time and production costs while preserving stringent performance criteria [9-10].

A crucial factor in this methodology is the clear differentiation between critical and non-critical surface zones.

Critical zones are areas where geometric deviation directly influences the product's function, safety, or assembly performance—examples include load-bearing interfaces, aerodynamic profiles, and precise joints. These areas demand stringent control and tighter tolerance limits [11].

Non-critical zones, on the other hand, have minimal effect on performance and often relate to secondary or aesthetic features. Applying relaxed tolerances to these areas reduces both fabrication costs and metrological complexity without compromising integrity [12-13].

Strategically distributing tolerance levels across components thus enables industries to balance accuracy, cost, and productivity. Furthermore, such optimization enhances communication between design engineers, production teams, and quality assurance, fostering a collaborative and adaptive manufacturing ecosystem [14].

By shifting from numerous local tolerances toward a unified global shape tolerance, companies can simplify their workflows, accelerate product validation, and minimize inspection redundancies [15]. Nonetheless, achieving this transformation requires careful calibration between precision demands and economic efficiency—tight tolerances for critical aerodynamic or structural zones and broader margins where permissible [16-17-18].

Implementation also depends on the evolution of digital tools, as CAD/CAM environments and metrology systems must be compatible with global tolerance models [19]. Advanced technologies such as artificial intelligence and machine learning provide valuable support by analyzing large datasets, identifying optimal tolerance distributions, and predicting manufacturing outcomes [20-[21]. In parallel, non-contact inspection techniques, including high-resolution 3D scanning and optical metrology, are crucial for verifying compliance within this framework [22-23].

Finally, international standards, notably ISO 1101, should evolve to incorporate these modern optimization principles [24]. By emphasizing the control of critical areas and leveraging intelligent inspection and manufacturing methods, this tolerance optimization paradigm promotes not only enhanced precision and efficiency but also environmental sustainability through reduced waste and optimized resource consumption. Ongoing research will need to validate these methods through industrial-scale case studies and advance AI-based optimization tools for broader industrial integration [25].

2 Modeling Framework for tolerance optimization in freeform geometries

2.1. Methodology

The optimization process for tolerances applied to freeform geometries follows a structured, multi-phase methodology. It begins by clearly defining the goals and scope of the study—chiefly, to reduce the total number of tolerances without compromising functional performance, product quality, or manufacturability. The initial stage involves a comprehensive data-gathering effort, encompassing CAD models, measurement data from FARO systems, and records of previous dimensional defects.

Once the dataset is established, the next step is geometric segmentation. This stage partitions the component's surface into distinct regions—classified as critical or non-critical—based on engineering analyses such as stress distribution studies or aerodynamic simulations. This classification provides the foundation for selective precision control across the geometry.

The core of the framework replaces numerous individual tolerance specifications with a unified global form tolerance. Within this scheme, high-priority zones receive more stringent control, while non-essential areas are permitted greater flexibility. This balance between accuracy and practicality is achieved through multi-objective optimization techniques—commonly employing algorithms such as particle swarm optimization—to minimize manufacturing costs, inspection effort, and geometric deviation simultaneously.

To enhance robustness and predictive capability, machine learning tools are integrated into the workflow. Regression-based and clustering models contribute to refining the distinction between surface categories and improving the accuracy of tolerance predictions.

Validation of the optimized tolerances is conducted through digital simulations and virtual inspections, wherein the refined tolerance framework is embedded directly within CAD environments. The results are then compared with baseline designs to quantify improvements in performance, manufacturability, and inspection efficiency.

The study culminates in a detailed case study illustrating practical implementation, followed by the formulation of comprehensive integration guidelines. These guidelines outline how optimized tolerances can be incorporated into both design and inspection workflows, promoting seamless adoption in industrial contexts and supporting scalability across diverse manufacturing applications.

2.2 .Modeling Tolerances for Freeform Geometries

In the tolerance optimization process, a cost function is employed as a central framework to establish an equilibrium between manufacturing precision, inspection effort, and geometric accuracy—particularly within critical regions. This function integrates three fundamental components:

the manufacturing cost, which reflects the resources required to achieve the desired tolerance levels,

the inspection cost, associated with measuring and verifying conformity to those tolerances, and

the geometric deviation in critical areas, which directly affects the part's functionality and overall performance.

By minimizing this cost function, it becomes possible to determine an optimal compromise that maintains a balance between precision and efficiency. The approach emphasizes tighter tolerances in critical zones—where deviations have the greatest impact—while permitting broader tolerance ranges in less critical regions. This strategy ensures high product reliability and manufacturability while significantly lowering total production and inspection costs.

The corresponding objective function can be expressed mathematically in Equation (1).

$$\mathrm{C} = \alpha \mathrm{C}_{\mathrm{man}} + \beta \mathrm{C}_{\mathrm{insp}} + \gamma \mathrm{D}_{\mathrm{crit}} \quad (1)$$

Where:

- $\mathrm{C}_{\mathrm{man}}$:Manufacturing cost related to tighter tolerances.
- $\mathrm{C}_{\mathrm{insp}}$: Inspection cost based on the complexity of the measurement process.
- $\mathrm{D}_{\mathrm{crit}}$: Deviation in critical zones.
- α, β, γ: Weight factors representing the importance of each term.

2.3 Constraints

- Geometric Deviation

The deviaion $D(x)$ must not exceed the allowed tolerance T for critical zones:

$$D(x) \leq T_{crit} \quad \forall \mathrm{x} \in \text{Critical zones} \quad (2)$$

For non-critical zones:

$$D(x) \leq T_{non-crit} \quad \forall \mathrm{x} \in \text{Non} - \text{Critical zones} \quad (3)$$

- Surface Continuity

$\frac{\partial T_x}{\partial x}$ is continuous, $\forall \mathrm{x} \in$ Interface Regions

- Manufacturing Constraints

Tolerance values must be within the limits achievable by the maufacturing process:

$$T_{min} \leq T(x) \leq T_{max} \quad (4)$$

3 Optimization Process for Tolerances in Freeform Geometries

3.1. Optimization Algorithm

The Particle Swarm Optimization (PSO) algorithm was selected for this study due to its proven ability to efficiently address complex, multidimensional optimization problemsparticularly those involving trade-offs between manufacturing expenses, inspection difficulty, and geometric deviation in freeform surfaces.
Drawing inspiration from the collective movement and decision-making patterns observed in bird flocks, PSO operates through a population of individual "particles," each representing a potential solution. These particles move within the search space, continuously updating their positions based on both their own experience (personal best) and the best performance achieved by the entire swarm (global best).
This adaptive mechanism enables a balanced exploration and exploitation of the solution domain, promoting convergence toward an optimal global solution. In the context of this work, PSO is applied to minimize a comprehensive cost function that integrates manufacturing and inspection costs together with deviation measures in critical zones.

Through successive iterations, the algorithm refines tolerance values across both critical and non-critical regions, achieving an optimized balance between precision, cost, and manufacturability.

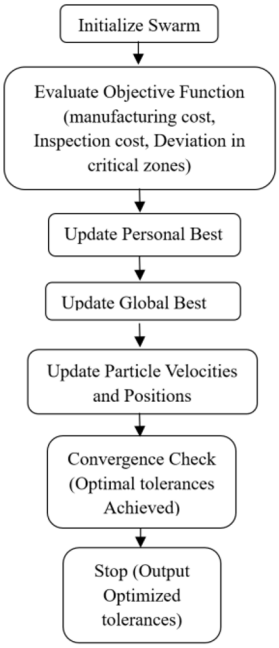

Fig. 1. PSO Process for Tolerance Optimization in Freeform Geometries

Figure 1 presents the workflow of the Particle Swarm Optimization (PSO) method applied to tolerance optimization. The process begins with the initialization of a swarm of particles, where each particle symbolizes a potential solution within the search domain. Each candidate solution is then assessed using a cost function that accounts for manufacturing and inspection expenses, as well as geometric deviations occurring in critical zones.During each iteration, the algorithm updates both the individual best (personal best) and the collective best (global best) solutions, using these references to adjust particle velocities and positions. This iterative refinement progressively directs the swarm toward the region of optimal solutions. The cycle continues until the convergence condition is satisfied, resulting in a set of optimized tolerance values that achieve a balanced trade-off between accuracy, production cost, and functional performance.Overall, the flowchart underscores the systematic and adaptive nature of PSO, demonstrating its effectiveness in tackling the inherently complex challenge of tolerance optimization with both precision and efficiency.

3.2. Case study

The turbine blade examined in this study represents a key element in both aerospace and energy-generation systems. Its freeform geometry demands exceptional precision during manufacturing and quality verification to guarantee optimal aerodynamic and structural performance. Within this component, certain regions—particularly the leading and trailing

edges—are classified as critical zones because even minor geometric deviations can significantly affect efficiency, reliability, and safety. In contrast, the central region of the blade, being less sensitive to aerodynamic variation, allows for slightly greater dimensional flexibility.

To assess conformity, measurements are carried out using a FARO arm, a high-precision non-contact inspection tool. A denser network of measurement points is strategically assigned to the critical areas to accurately capture fine geometric deviations, while a sparser distribution is sufficient for non-critical surfaces. This selective approach reduces both inspection time and associated costs without compromising accuracy.

Figure 2, titled Measurement Point Distribution for the Turbine Blade Using FARO Arm, illustrates this optimized balance, emphasizing how a tailored measurement strategy can enhance both functional integrity and overall efficiency in inspection processes.

Fig. 2. Measurement Point Distribution for the Turbine Blade Using FARO.

The turbine blade analyzed in this work serves as a vital element in both aerospace propulsion and power generation systems. Its complex freeform geometry necessitates extremely high manufacturing accuracy and rigorous quality assurance to meet performance and safety requirements. Within this geometry, critical regions—notably the leading and trailing edges—require particularly tight tolerances to maintain aerodynamic efficiency and structural integrity. Conversely, non-critical areas, such as the central portion of the blade, can accommodate slightly larger deviations without impairing functionality.

During inspection, a FARO arm is employed to perform precise three-dimensional measurements. To ensure accuracy while optimizing time and cost, a denser set of measurement points is strategically concentrated in the critical zones, whereas fewer points are used in the less sensitive regions. This adaptive measurement strategy achieves a practical balance between precision, efficiency, and inspection economy.

Such a balanced distribution of measurement points ensures both functional reliability and process optimization, as illustrated in the corresponding turbine blade model.

Table 1. MEASUREMENT POINT DISTRIBUTION FOR THE TURBINE

Zone	Criticality	Number of Measurement Points	Purpose
Leading Edge	High	150	Ensure aerodynamic precision
Trailing Edge	High	150	Ensure aerodynamic precision
Central Region	Medium	80	Capture surface deviations
Base	Medium	60	Verify dimensional conformity
Tip	Low	50	Verify overall geometry

Table 1 summarizes the allocation of measurement points across the various regions of the turbine blade according to their level of criticality and functional importance. The leading and trailing edges, identified as high-criticality zones due to their direct influence on aerodynamic performance, receive the greatest concentration of measurements 150 points each—to ensure exceptional geometric accuracy. The central region, categorized as moderately critical, is assigned 80 points to effectively capture surface deviations that could affect flow continuity. Meanwhile, the base and tip areas, characterized by medium and low criticality respectively, are inspected using a smaller number of point 60 and 50 sufficient to confirm dimensional consistency and general geometric integrity. This measurement distribution embodies a balanced inspection strategy: it concentrates resources and precision efforts on the most performance-sensitive regions while maintaining efficiency by reducing measurement density in less critical zones.

4 Results and discussion

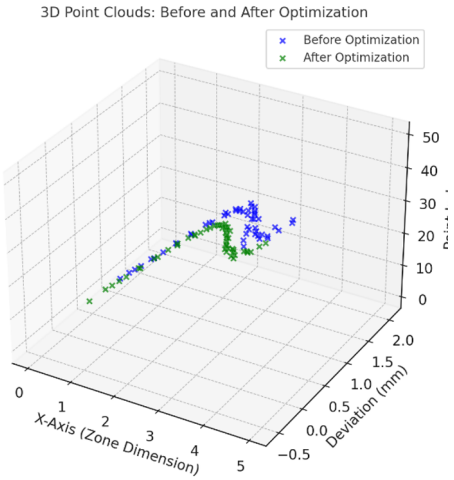

Fig. 3. 3D point clouds

Figure 3 illustrates the point cloud representations of the turbine blade both before and after the tolerance optimization process. In this visualization, the blue points correspond to the initial deviations identified during the inspection phase, whereas the green points depict the reduced deviations obtained following the application of the optimization method.

A clear reduction in deviation magnitude can be observed, particularly within the critical regions, indicating a significant improvement in geometric precision. Meanwhile, non-critical zones maintain acceptable variation levels, ensuring that inspection and manufacturing efficiency are preserved.

Overall, this visualization effectively demonstrates the capability of the optimization approach to align the actual blade geometry more closely with its intended design specifications, thereby validating the efficiency of the proposed methodology.

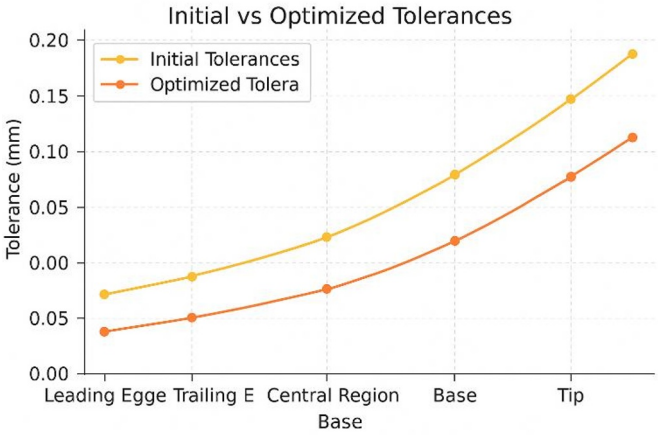

Fig. 4. Initial vs Optimized Tolerances

Figure 4 presents a comparative visualization of the turbine blade's tolerance distribution before and after optimization, revealing a consistent reduction in tolerance values across all surface zones. The critical regions—notably the leading and trailing edges—show the most pronounced improvements, confirming enhanced geometric precision essential for maintaining optimal aerodynamic performance.

In contrast, the non-critical areas, such as the base and tip, display more moderate reductions, aligning with their lower functional sensitivity and relaxed tolerance criteria. This differentiated improvement pattern illustrates the efficiency of the optimization strategy in concentrating precision where it has the greatest impact.

The resulting balance between performance assurance and cost efficiency demonstrates the robustness of the optimization process, which successfully enhances functionality while minimizing overall manufacturing and inspection expenditures.

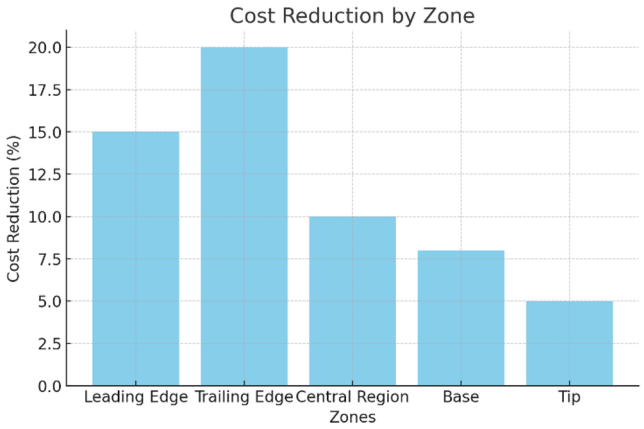

Fig. 5. Cost Reduction by Zone

Figure 5 illustrates the percentage reduction in manufacturing costs obtained following the implementation of the tolerance optimization procedure. The most substantial decreases are observed in the critical regions—specifically the leading and trailing edges—where enhanced precision and optimized allocation of production resources contribute to significant cost savings.

Conversely, the non-critical zones, such as the base and tip, exhibit more modest reductions, consistent with their comparatively lower influence on total manufacturing expenses.

Overall, these results underscore the effectiveness of the optimization framework in achieving a balanced compromise between economic efficiency and functional performance, ensuring that cost reductions do not come at the expense of component reliability or quality.

Figure 6, titled Inspection Time Reduction by Zone, illustrates a marked decrease in inspection duration across all regions of the turbine blade following the tolerance optimization process. The critical areas—notably the leading and trailing edges—display the most pronounced reductions, demonstrating that inspection activities have been significantly streamlined without compromising measurement accuracy.

Similarly, the non-critical zones, including the base and tip, reveal considerable time savings, highlighting the benefits of concentrating inspection resources on functionally significant regions.

Overall, this outcome confirms the effectiveness of the optimization approach in reducing inspection complexity and enhancing operational efficiency, thereby contributing to a more balanced and resource-efficient quality control process.

The optimization process resulted in a noticeable reduction of tolerance values across all regions of the turbine blade. In the critical zones—such as the leading and trailing edges—tolerances were significantly tightened, thereby improving aerodynamic performance and overall functional accuracy. In contrast, the non-critical areas were assigned more relaxed tolerances, effectively reducing manufacturing expenses and inspection duration without impacting operational efficiency.

This optimized distribution demonstrates a successful balance between precision enhancement and process efficiency. However, additional validation is recommended to confirm that the relaxation of tolerances in less critical regions does not adversely affect the long-term structural integrity or durability of the component under operational conditions.

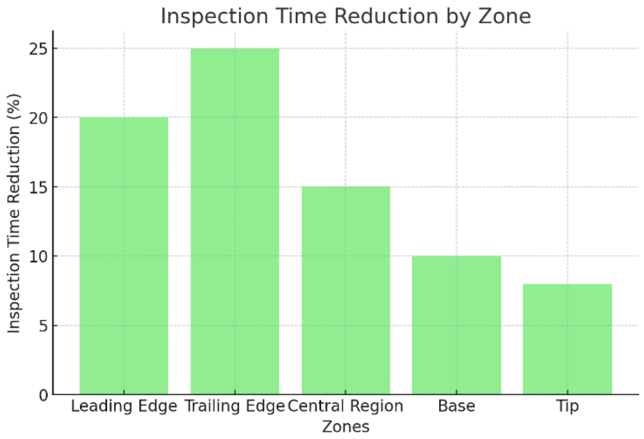

Fig. 6. Inspection Time Reduction by Zone

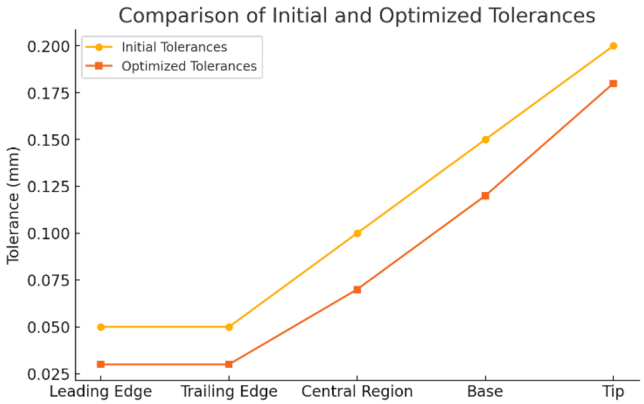

Fig. 7. Comparison of Initial and Optimized Tolerances

5 Conclusion

This research demonstrates the strong potential of the Particle Swarm Optimization (PSO) algorithm for enhancing tolerance optimization in complex freeform geometries, as exemplified by turbine blade applications. By transitioning from numerous localized tolerance definitions to a unified global optimization framework, the proposed methodology achieves an effective equilibrium between geometric precision, cost efficiency, and inspection simplicity.

In this optimized configuration, high-criticality regions—notably the leading and trailing edges—are assigned tighter tolerance limits to ensure aerodynamic accuracy and structural functionality. Conversely, non-critical zones benefit from more flexible tolerance settings, which significantly reduce manufacturing effort and inspection workload without compromising overall performance.

The results indicate substantial decreases in both production cost and inspection time, emphasizing the practical relevance of this approach for advanced manufacturing sectors such as aerospace and power generation. Nonetheless, further investigations are recommended to evaluate long-term structural reliability and to explore the scalability of this optimization framework for more complex geometries and large-scale industrial integration.

References

1. Hosseini, S.E.; Jafaripanah, S.; Saboohi, Z. Numerical Simulation and Aerodynamic Optimization of Two-Stage Axial High-Pressure Turbine Blades. arXiv 2024, arXiv:2401.02102.
2. Geneid, A.A.; Atia, M.R.A.; Badawy, A. Multi-objective optimization of vertical-axis wind turbine's blade structure using genetic algorithm. J. Eng. Appl. Sci. 2022, 69, 137–149.
3. A. El-Nemr, E.A. Ahmed, C. Barris, B. Benmokrane, "Bond-dependent coefficient of glass- and carbon-FRP bars in normal- and high-strength concretes," Constr. Build. Mater., 113, 77–89 (2016)
4. Ahmadi, P.; Rashidi, M.M.; Nazari, M.A. Aerodynamic Optimal Design of Wind Turbine Blades using Genetic Algorithm. Int. J. Energy Environ. Eng. 2014, 5, 373–380.
5. O. Gouda, A. Hassanein, K. Galal, "Experimental and numerical study on the crack width and deflection performance of GFRP reinforced concrete beams," Eng. Struct., 283, 115721 (2023)
6. Rashidi, M.M.; Ahmadi, P.; Nazari, M.A. Optimization of blade profile for a horizontal axis wind turbine using genetic algorithm. Energy Convers. Manag. 2013, 70, 147–155.
7. Jafaripanah, S.; Hosseini, S.E.; Saboohi, Z. Aerodynamic optimization of a two-stage axial high-pressure turbine using genetic algorithm. Energy 2022, 238, 46–57.
8. E. B. Moreira, J. de J. A. Baldovino, and R. L. dos S. Izzo, "Transforming Construction and Demolition Waste into Soft-Soil Treatment for Paving Design," Jun. 18, 2023, Springer Science+Business Media. doi: 10.1007/s10706- 023-02503-8
9. Pholdee, N.; Bureerat, S. Hybrid evolutionary algorithms for structural optimization: A review. Comput. Struct. 2014, 139, 1–16.
10. G. Dana Boca and S. Saraçlı, "Environmental Education and Student's Perception, for Sustainability," Mar. 14, 2019, Multidisciplinary Digital Publishing Institute. doi: 10.3390/su11061553.
11. B. McCallum, "Experimental evaluation of the bond dependent coefficient and parameters which influence crack width in GFRP reinforced concrete," M.A.Sc. thesis, Dalhousie University, Canada (2013)
12. Verstraete, T.; Muller, L.; Mueller, J.D. CAD-Based Adjoint Optimization of the Stresses in a Radial Turbine. In Proceedings of the ASME Turbo Expo 2017, Charlotte, NC, USA, 26–30 June 2017.
13. Zielinski, M.; Ziller, G. Noncontact vibration measurements on compressor rotor blades. Meas. Sci. Technol. 2000, 11, 847–856. [CrossRef]
14. Brandstetter, C.; Schneider, A.P.; Fiquet, A.-L.; Paoletti, B.; Billon, K.; Ottavy, X. ECL5/CATANA: ECL5/CATANA: Comparative Analysis of Advanced Blade Vibration Measurement Techniques. In 16th European Turbomachinery Conference, paper n◦ ETC2025-176, Hannover, Germany, 24–28 March 2025. Avaliable online:

https://www.euroturbo.eu/publications/conferenceproceedings-repository/ (accessed on 20 June 2025)

15. Franke, D.; Jüngst, M.; Möller, D.; Schiffer, H.-P.; Giersch, T. Influence of pre-swirl, rotor speed and blade count on aeroelastic coupling mechanisms during stall inception of a transonic compressor. In Proceedings of the Turbo Expo: Power for Land, Sea, and Air, Online, 21–25 Septembre 2020; GT2020-14105 9p.
16. Bartolo, P. Stereolithographic Processes. In Stereolitography: Materials, Processes and Applications; Bartolo, P., Ed.; Springer: Boston, MA, USA, 2011; pp. 1–36.
17. S. Mehany, H.M. Mohamed, A. El-Safty, B. Benmokrane, "Bond-dependent coefficient and cracking behavior of lightweight self-consolidating concrete (LWSCC) beams reinforced with glass- and basalt-FRP bars," Constr. Build. Mater., 329, 127130 (2022)
18. Lawson, C.; Ivey P. Turbomachinery blade vibration amplitude measurement through tip timing with capacitance tip clearance probes. Sens. Actuators A Phys. 2005, 118, 14–24. [CrossRef]
19. I. N. Permadi and D. B. Nisa, "A Model Experiment Design Using the Taguchi Method: A Case Study Of Making Concrete Roof," May 31, 2023. doi: 10.59976/jurit.v1i1.2.
20. Pietropaoli, M.; Ahlfeld, R.; Montomoli, F.; Ciani, A.; d'Ercole, M. Design for Additive Manufacturing: Internal Channel Optimization. J. Eng. Gas Turbines Power 2017, 139, 102101. [CrossRef]
21. Stapelfeldt, S.; Brandstetter, C. Suppression of Nonsynchronous Vibration Through Intentional Aerodynamic and Structural Mistuning. J. Turbomach. 2022, 144, 021008. [CrossRef]
22. Kielb, R.; Barter, J.; Thomas, J.; Hall, K. Blade excitation by aerodynamic instabilities: A compressor blade study. In Proceedings of the Turbo Expo: Power for Land, Sea, and Air, Atlanta, GA, USA, 16–19 June 2003; GT2003-38634, pp. 399–406.
23. Lee, J.; Francis, J.M.; Wang, L.M. How tonality and loudness of noise relate to annoyance and task performance. Noise Control. Eng. J. 2017, 65, 71–82. [CrossRef]
24. Haddi, Y.; Moumen, A.; Kharchaf, A. Study of A Mobile Robot's Obstacle Avoidance Behavior in A Radioactive Environment with A High Level of Autonomy. Int. J. Tech. Phys. Probl. Eng. (IJTPE) 2022, 14, 34–41.
25. Moumen, A.; Lakhdar, A.; Mansouri, K. Elastoplastic Behavior of Polybutylene Terephthalate Polyester Bio loaded by Two Sustainable and Ecological Fibers of Animal Origin with Two Numerical Methods. Int. J. Tech. Phys. Probl. Eng. (IJTPE) 2021, 13, 29–37.